

JPE 8-3-3

Design, Implementation and Testing of HF transformers for Satellite EPS Applications

Mohamed Zahran[†][†]Electronics Research Institute, Cairo, Egypt

ABSTRACT

The electric power subsystems (EPS) of most remote sensing satellites consist of a solar array as a source of energy, a storage battery, a power management and control (PMC) unit and a charge equalization unit (CEU) for the storage battery. The PMC and CEU use high frequency transformers in their power modules. This paper presents a design, implementation and testing results of a high frequency transformer for the EPS of satellite applications. Two approaches are used in the design process of the transformer based on the pre-determined transformer specifications. The transformer is designed based on an ETD 29 ferrite core. The implemented transformer consists of one center-tapped primary coil with eleven center-tapped secondary coils. The offline calculation results and measured values of R, L for transformer coils are convergence. A test circuit for measuring the transformer parameters like voltage, current and B-H hysteresis was implemented and applied. The test results confirm that the voltage waveforms of both primary and secondary coils were as desired. No overlapping occurred between the control signal and the transformer, which was not saturated during testing even during a short circuit test of the secondary channels. The dynamic B-H loop characteristics of the used transformer cores were measured. The sample test results are given in this paper.

Keywords: HF Transformers, Ferrite cores, ETD Cores, Satellite Power Systems

1. Introduction

Static inverters, converters and transformer-rectifier (T-R) supplies intended for spacecraft power use are usually created in a square loop toroidal design. The design of reliable, efficient and lightweight devices of this class for such use has been seriously hampered by the lack of engineering data describing the behavior of both the

commonly used and the more exotic core materials with higher frequency square wave excitation. The magnetic materials are studied by ^[1] for use in spacecraft transformers used in static inverters, converters, and transformer rectifier supplies.

Transformers used for inverters, converters and T-R supplies operate from the spacecraft power bus which is usually in DC. One important consideration affecting the design of suitable transformers is that care must be taken to ensure that operation involves a balanced drive to the transformer primary. In the absence of a balanced drive, a net DC current will flow in the transformer primary, which causes the core to saturate easily during alternate

Manuscript received Jan. 7, 2008; revised April 8, 2008

[†]Corresponding Author: Zahran@eri.sci.eg
Tel: +202-26225821, Fax: +202-26225833
Electronics Research Institute, Cairo, Egypt

half-cycles. A saturated core cannot support the applied voltage, and because of lowered transformer impedance the current flowing in a switching transistor is limited only by its beta. Transformer leakage inductance results in a high voltage spike during the switching sequence which could be destructive to the transistors [1]. In order to provide a balanced drive, a push-pull power circuit controlled by a PWM signals (symmetrical drive for both sides of the transformer primary winding) is used in the application presented in this paper.

2. Transformer Specification

The specification of transformer is determined by the application in which the transformer is used. Unlike [2], the transformer design considerations dealt with in this publication are:

- Maximum power level to be handled,
- Frequency range,
- Input & output needed voltages (turns ratio),
- Allowable control signal,
- Duty cycle of signal operation,
- Core type, shape and material properties.

The following information is the design specification for a push-pull transformer, operating at 30 kHz, using the Kg core geometry approach. For a typical design example, assume a push-pull, full-wave, center-tapped circuit, as shown in Fig. 1 [3], [4].

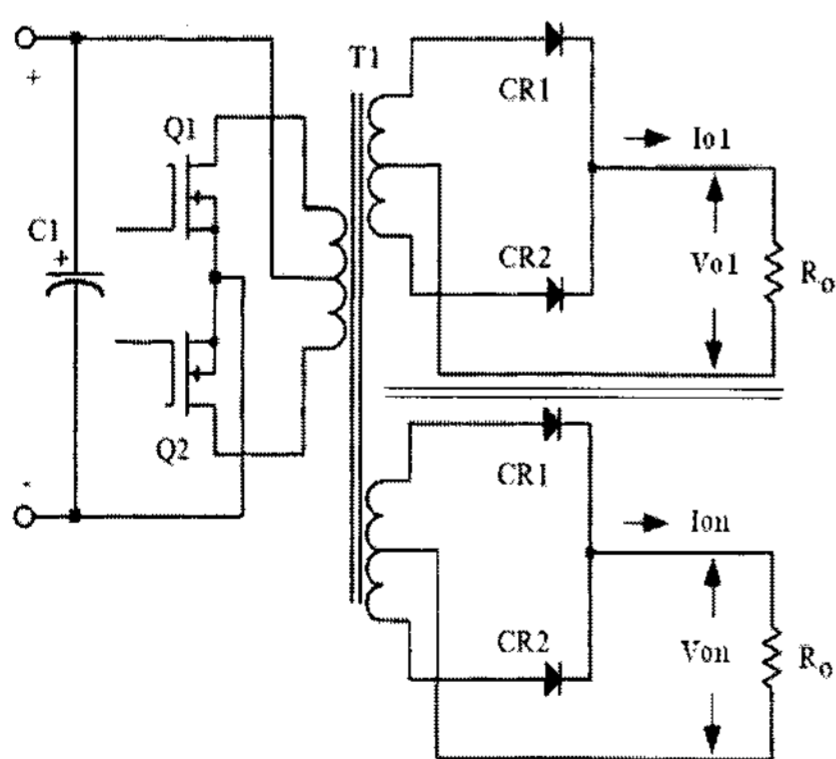


Fig. 1 Multiple Output Converter

Table 1 illustrates the design transformer parameters (specification).

Table 1 Design parameters of the transformer

Parameter	Symbol	Value & unit
1. Input voltage,	V_p	= 20 volts
2. Output voltage # 1,	V_{O1}	= 1.2 volts
3. Output current # 1,	I_{O1}	= 6.0 amps
4. Output voltage # n,	V_{On}	= 1.2 volts
5. Output current # n,	I_{On}	= 6.0 amps
6. Frequency,	f	= 30kHz
7. Efficiency,	η	= 98%
8. Regulation,	α	= 0.5%
9. Diode voltage drop,	V_d	= 1.0 volt
10. Operating flux density,	B_{ac}	= 0.1 Tesla
11. Window utilization,	K_u	= 0.4
12. Temperature rise goal,	T_r	= 30°C
13. Summation of Output Current	$\sum_1^{22} I_{O-max}$	= 10A

3. Transformer Design Approaches

Two design approaches for designing the HF transformer based on the core geometry are introduced by Colonel WM. T. McLyman [3], and R.W. Erickson [5].

These two approaches are applied in this case study, the design steps as well as results are shown in the following two sections. The results of both will be analyzed and confirmed with the experimental results.

3.1 First Design Approaches

Colonel WM. T. McLyman reported in [3] a detailed and well defined procedure for the design of an HF transformer for a different application. The application of this approach is illustrated in the following 28 steps:

Step 0 : Selection of Wire Diameter

At this point, select a wire so that the relationship between the AC resistance and the DC resistance is;

$$\frac{R_{AC}}{R_{DC}} = 1$$

The skin depth, ϵ , in centimeters, is:

$$\epsilon = \frac{6.62}{\sqrt{f}} = 0.038 \text{ cm} \quad (1)$$

Then, the wire diameter, DAWG is:

$$D_{AWG} = 2. \varepsilon = 0.0764 \quad (2)$$

Then, the bare wire area, A_w , is:

$$A_w = \frac{\pi \cdot (D_{AWG})^2}{4} = 4.5 \cdot 10^{-3} \text{ cm}^2 \\ = 0.45 \text{ mm}^2 \quad \text{Practically we use } 0.5 \text{ mm}^2$$

From the section of Wire-Table (Table 2), wire number 2 has a bare wire area of 0.005188 centimeters square. This will be the minimum wire size used in this design. If the design requires more wire area to meet the specifications, then the design will use a multiplier of #2.

Table 2 Wire Table

AWG	bare	Area $\text{cm}^2 \cdot 10^{-3}$	nce $\mu\Omega/\text{cm}$	Area $\text{cm}^2 \cdot 10^{-3}$	Diamet er cm	Turns per cm	Turns per cm^2	Weight gm/cm
1	6.531	263.9	7.539	0.0980	10.2	80	0.05940	
2	5.188	332.3	6.065	0.0879	11.4	99	0.04726	
3	4.116	418.9	4.837	0.0785	12.8	124	0.03757	
4	3.2430	531.4	3.8570	0.0701	14.3	156	0.02965	
5	2.5880	666.0	3.1350	0.0632	15.8	191	0.02372	

Step 1 : Calculate the transformer output power, P_o

$$P_o = P_{o1} + P_{o2} + \dots + P_{on} \\ = \sum_1^{22} I_o \cdot (V_o + V_D) = 22 \text{ W} \quad (3)$$

Step 2 : Calculate the total secondary apparent power, P_{ts} .

$$P_{ts} = P_o \cdot U \quad (4)$$

Notes:

- Using a center-tapped winding, $U = 1.41$
- Using a single winding, $U = 1.0$

$$P_{ts} = 31.02 \text{ W}$$

Step 3 : Calculate the total apparent power, P_t .

$$P_t = P_{tp} + P_{ts} = \frac{P_o}{\eta} \cdot U + P_{ts} = 62.67 \text{ W} \quad (5)$$

Step 4 : Electrical conditions Calculation, K_e

$$K_e = 0.145 \cdot K_f^2 \cdot f^2 \cdot B_m^2 \cdot 10^{-4} = 2088 \quad (6)$$

Step 5 : Calculate the core geometry, K_g .

$$K_g = \frac{P_t}{2 \cdot K_e \cdot \alpha} \text{ cm}^3$$

With operation at 30 kHz, and because of the skin effect, the overall window utilization, K_u , is reduced. To return the design back to the norm, the core geometry, K_g , is to be multiplied by 1.35,

$$K_g = \frac{P_t}{2 \cdot K_e \cdot \alpha} \cdot 1.35 = \frac{62.67 \cdot 1.35}{2 \cdot 2088 \cdot 0.5} = 0.0405 \text{ cm}^3 \quad (7)$$

Step 6 : Select an ETD core

From the data base in [3], [5], the relevant core types are; EE43208, EC35, ETD29, ETD39(lp), PQ26/20, RM-10, and many others. In this application, an ETD29 core is used, and the following design steps can be completed.

Step 7 : Calculate the number of primary turns, N_p , using Faraday's Law.

$$N_p = \frac{V_p \cdot 10^4}{K_f \cdot B_{ac} \cdot f \cdot A_c} \quad (8)$$

$$N_p^{ETD-29} = 21.9 \cong 22 \text{ Turns}$$

Step 8 : Calculate the current density, J ,

Using a window utilization, $K_u = 0.29$.

$$J = \frac{P_t \cdot 10^4}{K_f \cdot K_u \cdot B_{ac} \cdot f \cdot A_p} \quad (9)$$

$$J_{ETD-29} = 1.6675 \text{ A/mm}^2,$$

It should be noted that K_g for ETD29 > desired K_g by more than 30%, so J_{ETD-29} can be considered at least:

$$J_{ETD-29} = 2.875 \text{ A/mm}^2$$

Step 9 : Calculate the input current, I_{in} :

$$I_{in} = \frac{P_o}{V_{in} \cdot \eta} = 1.122 \text{ A} \quad (10)$$

Step 10 : Calculate the primary bare wire area, $A_{WP(B)}$:

$$A_{WP(B)} = \frac{I_{in} \cdot \sqrt{D}}{J} \quad (11)$$

$$A_{WP(B)-Dmax}^{ETD-29} = 0.262 \text{ mm}^2,$$

$A_{WP(B)-Dmin}^{ETD-29} = 0.214mm^2, 0.5mm^2$ is used.

Step 11 : Calculate the required number of primary strands, Snp.

$$Snp = \frac{A_{WP(B)}}{\text{Bare Area of wire \#2}} \quad (12)$$

for Dmax Snp=0.87, for Dmin Snp=0.71

In practice, the equation Snp = 1 is applied.

Step 12 : Calculate the primary $\mu\Omega/cm$

$$\mu\Omega/cm = \frac{\mu\Omega/cm}{Snp} = 332.3 \quad (13)$$

Step 14 : Calculate the primary resistance, Rp.

$$R_p = MLT * N_p * \left(\frac{\mu\Omega}{cm}\right) * 10^{-6} \quad (14)$$

$$R_p^{ETD-29} = 0.04678\Omega$$

Step 14 : Calculate the primary copper loss, Pp.

$$P_p = I_p^2 * R_p \quad (15)$$

$$P_p^{ETD-29} = 0.05889 W$$

Step 15 : Calculate the secondary turns, Ns1,..n

$$N_{S1,..n} = \frac{N_p * V_{S1}}{V_p} * \left(1 + \frac{\alpha}{100}\right) \quad (16)$$

$$N_{S1,..n}^{ETD-29} = 2.09 \text{ Turns}$$

Taking into account the 0.7V diode voltage drop, in practice the number of turns of the secondary winding is 2 turns while the number of turns of the primary winding is 22 turns.

$$N_p = 22 \text{ Turns} \quad \text{and} \quad N_s = 2 \text{ Turns}$$

Step 16 : Calculate the secondary bare wire area, A_{WS1}.

$$A_{WS1} = \frac{I_o \sqrt{D}}{J} \quad (17)$$

$$A_{WS1:D=0.45}^{ETD-29} = 0.0139cm^2, \quad A_{WS1:D=0.3}^{ETD-29} = 0.0114cm^2$$

Step 17 : Calculate the required number of secondary strands, S_{ns}.

$$S_{ns1} = \frac{A_{WS1}}{\text{wire \#2}} \quad (18)$$

$$S_{ns1:D=0.45}^{ETD-29} = 2.67, \quad S_{ns1:D=0.3}^{ETD-29} = 2.2$$

In practice, the number of secondary strands is taken only 2 times for possible implementation of the transformer with 11 secondary coils. Also, the maximum current is applied for a limited short period of time, although this rarely happens and then is distributed for multiple channels.

Step 18 : Calculate the secondary, S₁ new $\mu\Omega/cm$.

$$\mu\Omega/cm_{(new)} = \frac{\mu\Omega/cm}{S_{ns1}} = 166.45\mu\Omega/cm \quad (19)$$

Step 19 : Calculate the secondary S₁ resistance, R_{S1}.

$$R_{S1} = MLT * N_{S1} * \left(\frac{\mu\Omega}{cm}\right) * 10^{-6} \quad (20)$$

$$R_{S1}^{ETD-29} = 0.00213 \Omega$$

Step 20 : Calculate the secondary copper loss, P_s.

$$P_s = \sum I_s^2 * R_s \quad (21)$$

$$P_s^{ETD-29} = 0.213 W$$

Step 21 : Calculate the total primary and secondary copper loss, P_{cu}.

$$P_{CU} = P_p + P_s \quad (22)$$

$$P_{CU}^{ETD-29} = 0.2719 W$$

Step 22 : Calculate trans. regulation, α

$$\alpha = \frac{P_{CU}}{P_o} * 100 \quad (23)$$

$$\alpha^{ETD-29} = 1.236 \%$$

If regulation is reflected to secondary apparent power, p_{ts},

$$\alpha^{ETD-29} = 0.87 \%$$

Step 23 : Calculate the milli-watts per gram, mW/g.

$$\begin{aligned} \text{mW/g} &= 0.000318 * f^{1.51} * B_{AC}^{2.747} \\ &= 3.28 \text{ mW/g} \end{aligned} \quad (24)$$

Step 24 : Calculate the core loss, P_{fe}

$$P_{fe} = mW / g * W_{tfe} * 10^{-3} \quad (25)$$

$$P_{fe}^{ETD-29} = 0.0918 W$$

Step 25 : Calculate the total loss P_{Σ} ,

$$P_{\Sigma} = P_{fe} + P_{CU} \quad (26)$$

$$P_{\Sigma}^{ETD-29} = 0.3637 W$$

Step 26 : Calculate the watts per unit area,

$$\psi \text{ (W/cm}^2\text{)} = \frac{P_{\Sigma}}{A_t} \quad (27)$$

$$\psi^{ETD-29} = 0.008558,$$

Step 27 : Calculate the temperature rise, T_r

$$T_r = 450 * \psi^{0.826} \quad (28)$$

$$T_r^{ETD-29} = 8.817 ^\circ C,$$

3.2 Second Design Approach

R. W. Erickson reported in [5] that the design of an HF transformer can be summarized in the following four steps:

Step 1 : Core geometrical constant

$$K_{gfe} = \frac{\rho \cdot \lambda_1^2 \cdot I_{tot}^2 \cdot K_{fe}^{(2/B)}}{4 \cdot K_u \cdot (P_{tot})^{((B+2)/B)}} * 10^8 \quad (29)$$

Where:

ρ Wire effective resistivity ($\Omega - cm$), for copper
 $1.724 * 10^{-6}$

λ_1 Applied primary Volt-Second (V-Sec)

$$\lambda_1 = V_p T_S \cdot D \quad (30)$$

D Duty Cycle

V_p Primary Voltage (average during ON period)

TS = 1/(f/2) in case of single winding in primary and full wave,

= 1/f in case of center-tapped winding in primary

I_{tot} Total rms current referred to primary (A)

K_{fe} Core loss Coefficient ($W/cm^3 T^\beta$),
 $K_{fe} \cong 2.5 W/T^\beta \cdot Cm^3$

K_u Winding fill factor (0.3–0.5), Typical 0.4

B Core Loss Exponent (Typical =2.6)

Calculation of K_{gfe} parameters:

$$\lambda_1 = 200 V \cdot \mu - Sec$$

$$\bullet P_O = \sum_S I * V_S = 22W \quad (31)$$

$$\bullet n = V_p / (V_S + V_d) = 9 \quad (32)$$

$$\bullet \text{Allowed } P_{tot} = 0.5\% * P_O = 0.11W$$

$$\bullet I_{tot} = I_p + \frac{1}{n} \sum_S I_S = \frac{P_O}{\eta * V_p} + \frac{1}{n} \sum_S I_S = 2.235A \quad (33)$$

$$\bullet \text{Then; } K_{gfe} = 0.0021537$$

From the data base in [3] and [5], the relevant core types are; EE187, EE41805, EC35, ETD29, ETD34(lp), EFD20, PC41811, RM-6, and many others. In this application, the ETD29 core is used as the common selection in both approaches.

Step 2 : Evaluate peak AC flux density

$$\Delta B = \left\{ 10^8 * \frac{\rho \cdot \lambda_1^2 \cdot I_{tot}^2 * (MLT)}{2K_u \cdot W_A \cdot A_C^3 \cdot l_m \cdot \beta \cdot K_{fe}} * \frac{1}{\beta + 2} \right\} \quad (34)$$

Where for ETD-29 cores:

MLT Mean Length per Turn (cm), 6.4

W_A Core Window Area (cm²), 1.419

A_C Core crosses sectional area (cm²), 0.761

l_m Magnetic path length (MPL) (cm), 7.2, then,

$$\Delta B = \left\{ \frac{10^8 * 1.724 * 10^{-6} \cdot (200 * 10^{-6})^2 \cdot 2.23^2}{2 * 0.4} * \frac{(6.4)}{1.419 * 0.761^3 * 7.2} * \frac{1}{2.6 * 2.5} \right\} \quad (35)$$

$$= 0.0807119 Tesla$$

It should be noted that ΔB is less than operating flux density by means by which the core will not go into saturation during the handling of the desired power rating.

Step 3 : Evaluate the number of windings turns

$$n_p = \frac{\lambda_1}{2 \cdot \Delta B \cdot A_c} * 10^4, \quad n_s = n_p / n, \quad (35)$$

Then $n_p = 16.28, \quad n_s = 16.28 / 9 = 1.809$

Since n_s should be integer value,

$$n_s = 2 \text{ turns, then } n_p = 18 \text{ turns,}$$

Step 4 : Choose the wire size

$$\alpha_p = \frac{I_p}{n \cdot I_{tot}}, \quad A_{WP} = \frac{\alpha_p \cdot K_u \cdot W_A}{n_p} \quad (36)$$

$$\alpha_s = \frac{I_{s-rms}}{n \cdot I_{tot}}, \quad A_{WS} = \frac{\alpha_s \cdot K_u \cdot W_A}{n_s} \quad (37)$$

Where:

α_p, α_s Fraction of winding area assigned to primary and secondary,

A_{WP}, A_{WS} Winding cross sections area (cm^2)

$$\alpha_p = 0.0608, \quad A_{WP} = 0.192 \text{ mm}^2$$

$$\alpha_s = 0.163, \quad A_{WS} = 4.6 \text{ mm}^2$$

In cases where 0.5 mm^2 is used this means that:

$$S_{np} = 1, \text{ \& } S_{ns} = 9.$$

4. Analysis of the Two Design Approaches

The first approach illustrates a detailed step by step description of transformer design while the second one summarizes these in only four steps. Below shows a comparison between the two design approaches.

Table 3 Comparison between results of common parameters in two design approaches

Transformer Parameter	1 st approach	2 nd approach
Design reference	Core geometry	
Number of steps	28	4
Core type	ETD 29	
Flux Density	0.1T (assumed)	0.0807T (calculated)
N_p, S_{np}	22, 1	18, 1
N_s, S_{ns}	2, 2	2, 9
Wire type	Wire #2 (Table 2)	

The first approach gives logical accepted results in both

primary and secondary sides of the transformer either from number of turns or from number of strands.

In the second approach, it is clear that the number of secondary coils strands is unaccepted since it needs nine parallel wires in each coil side just to carry 6A using a wire of cross section area 0.5188 mm^2 . From an experimental point of view, it is impossible to have eleven center tapped coils with two turns each and nine parallel wires. However, second approach calculates the flux density and confirms that the transformer will not go into saturation during handling of the desired power.

As a result, the first approach was implemented.

5. Transformer Implementation

The design results shown in Table 3. They are used to implement the transformer based on the ETD-29. Figure 2 – Figure 4 shows the ETD-29 implemented transformer from different sides.

The implemented transformer has the following:

- One center-tapped primary coil with 22 turns,
- Eleven center-tapped secondary coils with double wires,
- ETD-29 core.

6. Transformer Verification

The implemented transformer is verified by measuring and calculating the transformer parameters. The coils inductances can be calculated using the formula ^[2]:

$$L = \mu_o \cdot \mu_r \cdot n^2 \cdot A / l \quad (38)$$

Where:

L = inductance in H

$\mu_o = 4 \pi * 10^{-7}$ (rationalized M.K.S. units)

μ_r = relative permeability

A = average ferrite cross section m^2

l = average length of the lines of force in m

n = turns ratio.

Table 4 shows the calculated and measured L & R values for the ETD-29 core based implemented transformer with the application of the first design approach results. The convergence between the measured and calculated values is very clear.

Table 4 Calculated & measured L, R for Primary and secondary coils

μ_r Values	Primary Inductances L_p mH		Primary Measured Resistance R_p		Secondary Inductances L_s mH		Secondary Measured Resistances R_s	
	Calc.	Meas.	Side of coil	two sides	Calc.	Meas.	Side of coil	two sides
1470	1.070	1.072	0.147	0.317	0.00798	0.008	0.037	0.045
1540	1.120	1.103	0.147	0.317	0.00836	0.009	0.037	0.045
1610	1.175	1.105	0.147	0.317	0.00874	0.009	0.037	0.045
		4.5 ¹				0.032 ²		

¹ (Total inductance for the center tapped primary coil), ²Total inductance for the center tapped secondary coil)

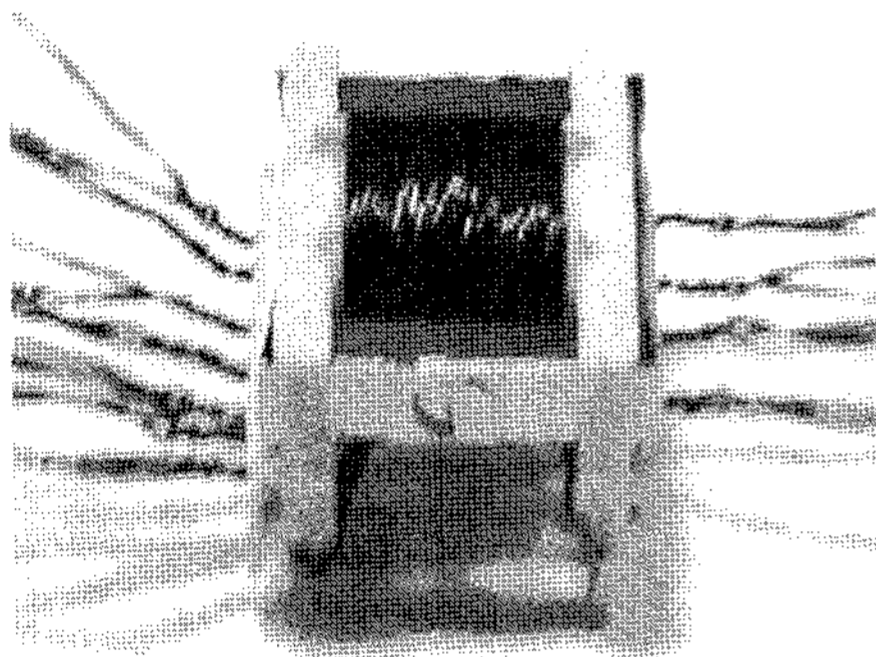


Fig. 2 Side View of transformer

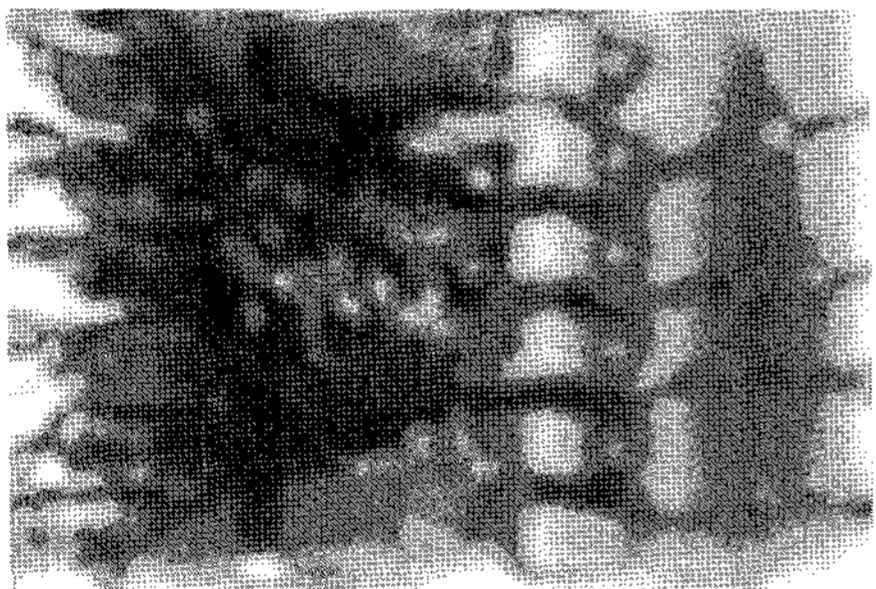


Fig. 3 Upside View of transformer

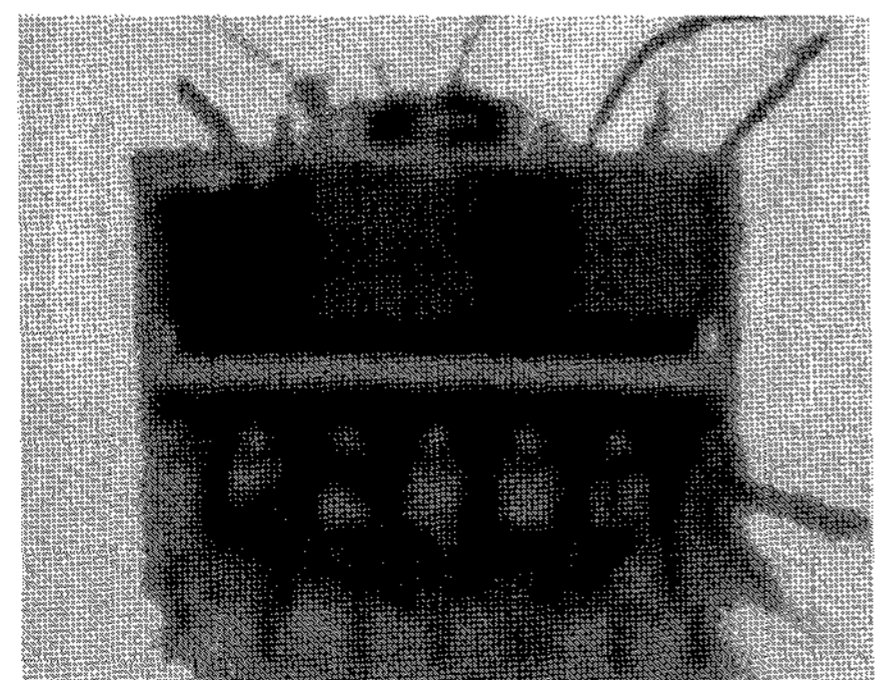


Fig. 4 Top View of transformer

7. Implemented Transformer Testing

7.1 B-H curves and Hysteresis Loop

For any given magnetic material, the relationship between the magnetizing force and the magnetic flux produced can be plotted. This is known as the B-H curve of the material, Fig. 5. From the B-H curve it can be seen that, as the magnetizing force is increased from zero, the flux increases up to a certain maximum value of flux. Above this level, further increases in magnetizing force results in no significant increase in the flux. The magnetic material is said to be 'saturated'.

A transformer is normally designed to ensure that the magnetic flux density is below the level that would cause saturation [6-10]. Along the initial magnetization curve at point X, the dashed line, in Fig. 6, B increases from the origin nonlinearly with H, until the material saturates. In practice, the magnetization of a core in an excited transformer never follows this curve, because the core is never in a totally demagnetized state, when the magnetizing force is first applied. The hysteresis loop represents energy lost in the core [3].

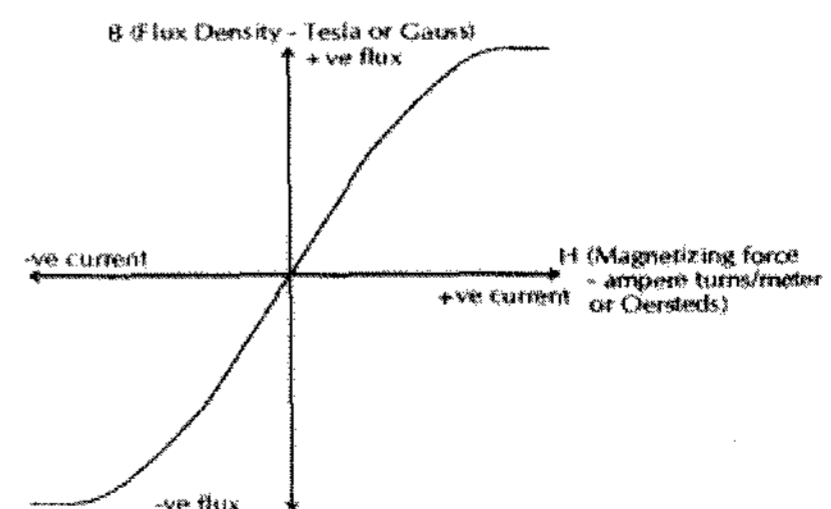


Fig. 5 B-H curve definition [6]

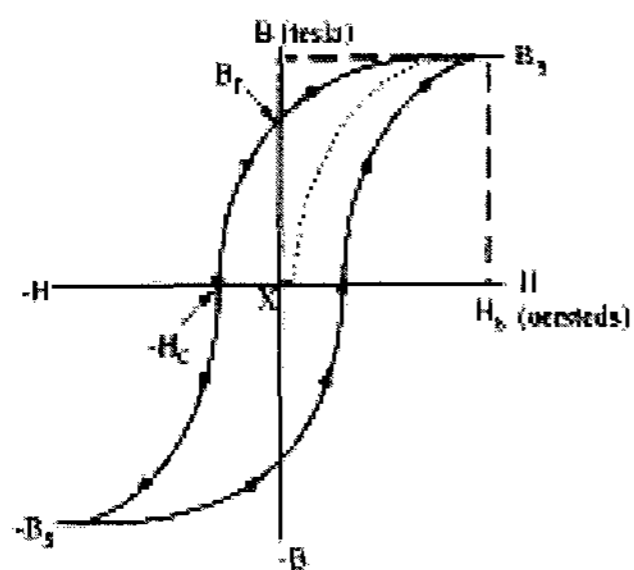


Fig. 6 Hysteresis loop of B-H Curve

7.2 Test Circuit of the B-H Loop

The test circuit is as shown in Fig. 7 [8]. The resistor R1 is kept small in comparison with the inductive reactance of the wound sample.

Field strength, H, is set by varying the current which is read as voltage across resistor R1.

Flux density of the cores is determined by integrating the secondary voltage using the RC circuit [8].

This relationship is displayed using the "X versus Y" display mode on an oscilloscope.

7.3 Measuring Parameters of B-H Loop

Magnetic terms are readily expressed in electrical terms to calibrate the display in units of Oersted (Oe) versus Gauss (G) [7]. Magneto -motive force is given by the equation [3]:

$$mmf = 0.4\pi NI, (\text{gilberts}) \quad (39)$$

Whereas mmf is the force, H is the force field, or force per unit length,

$$H = \frac{mmf}{MPL} = \frac{0.4\pi NI}{MPL} \left(\frac{\text{gilberts}}{\text{cm}} = \text{Oersted} \right) \quad (40)$$

$$H_{[Oe]} = \frac{0.4\pi * V_p * N_p}{MPL * R_1} \quad (41)$$

Normally, $2.0 < H_{oe} < 3.0$, $H \cong 2.5Oe$, then: $R1 \cong 20\Omega$

The flux density in Tesla can be deduced as follows:

$$\begin{aligned} \therefore E_{[V]} &= 4.0 * N_{[turns]} * f * \Phi_{[weber]} \\ &= 4.0 * N * f * B_{[T]} * A_{[m^2]} \end{aligned} \quad (42)$$

Since $f = 1/T$, and T is equal to the multiplication of the RC values (shown in Fig. 7), then flux density in Gauss can be obtained from the following formula:

$$B_{[G]} = \frac{R_2 * C * V_s}{N_s A_c [cm^2]} * 10^8 \quad (43)$$

Where:

R2, C is the integrating resistance, and capacitor.

Normally,

- $B \cong 0.1T_{(1000G)}$, then:
- $R_2 C \cong 0.722 * 10^{-5} s$
- If $C \cong 1\mu f$, Then $R_2 = 7.22\Omega$

7.4 HW set up for B-H Testing

The test circuit in Fig. 7 is implemented as shown in Fig. 8. The power amplifier module is built up based on the push-pull topology with IRF540 switches; the control signal is generated by a TL94 PWM generator. A digital storage oscilloscope is used in X-Y mode to plot the B-H curve at different conditions.

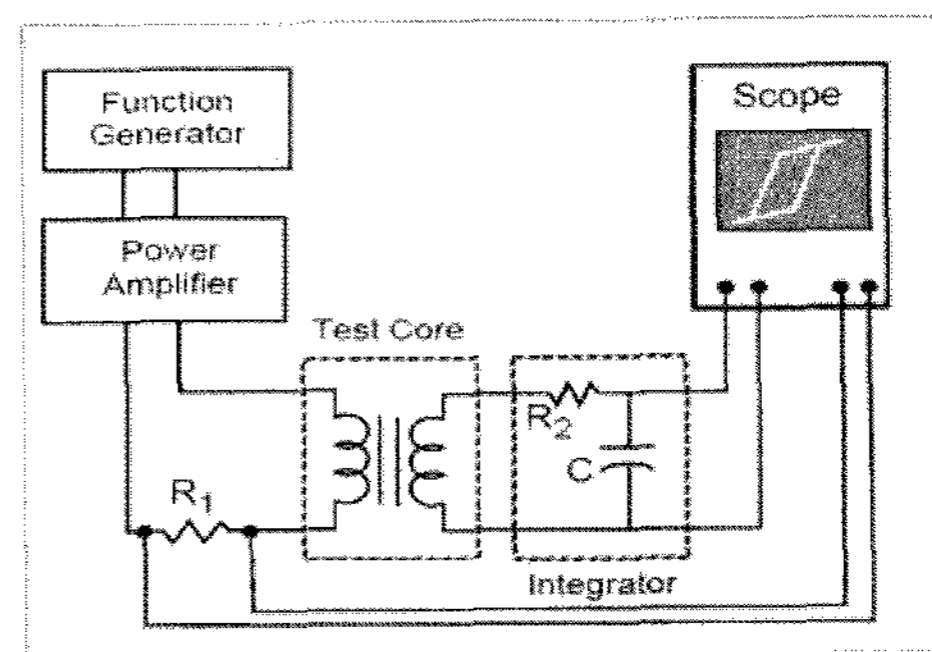


Fig. 7 Test set up of B-H Loop [11]

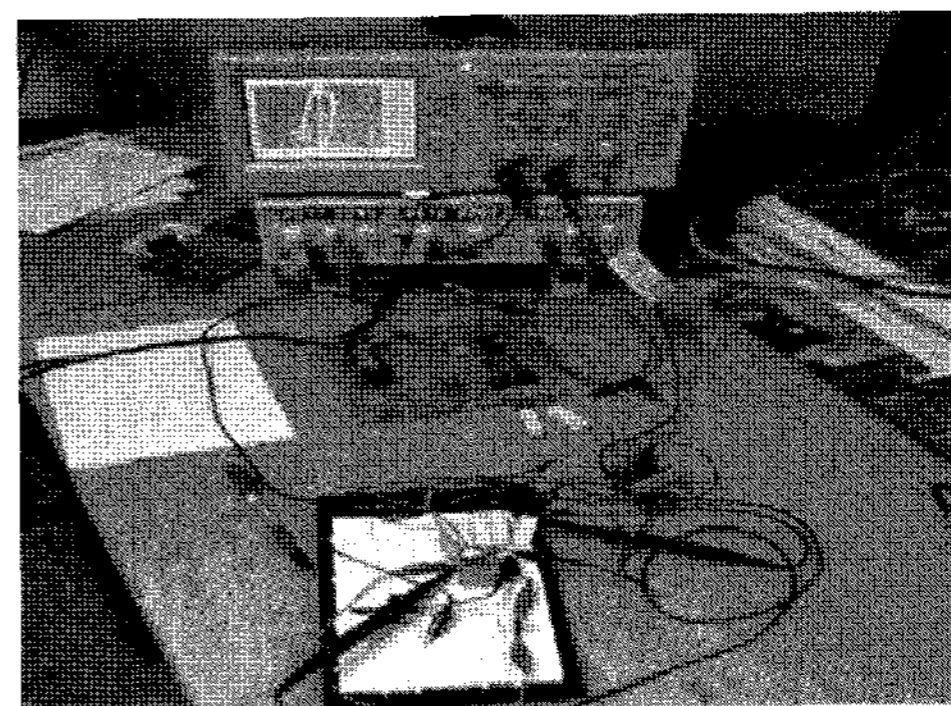


Fig. 8 B-H measuring HW

8. Experimental Results

Fig. 9 shows the primary voltage (two sides of coil) waveforms and Fig. 10 show a one side secondary voltage and current waveforms.

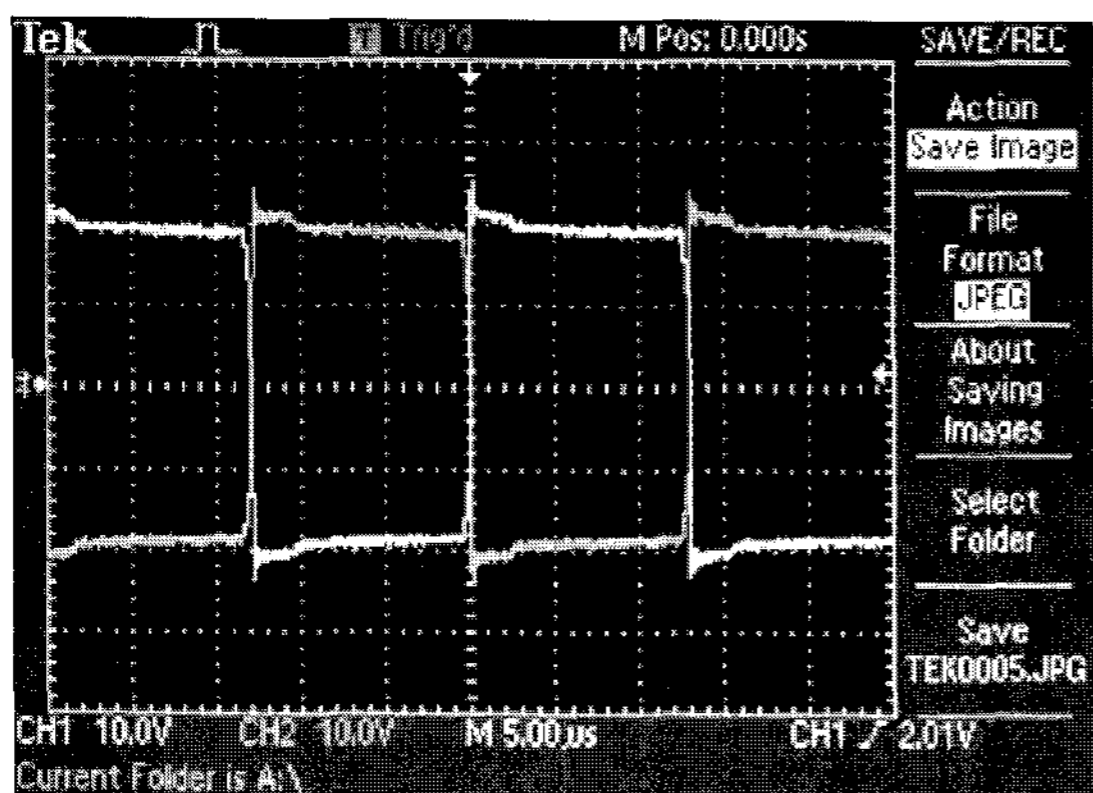


Fig. 9 Transformer Primary Voltages of Center Tapped Terminals, No Load

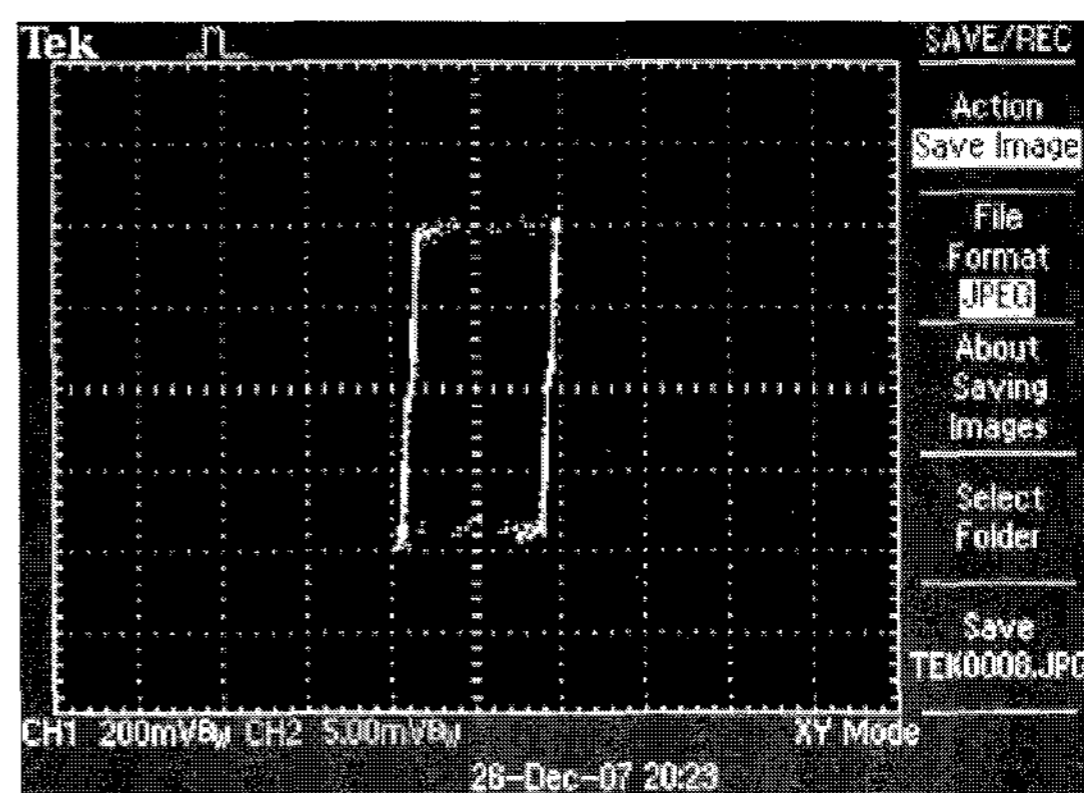


Fig. 12 B-H Curve, 45% Duty Cycle, $R_1=100\Omega$, $C=1\mu\text{F}$ Ceramic, No Load

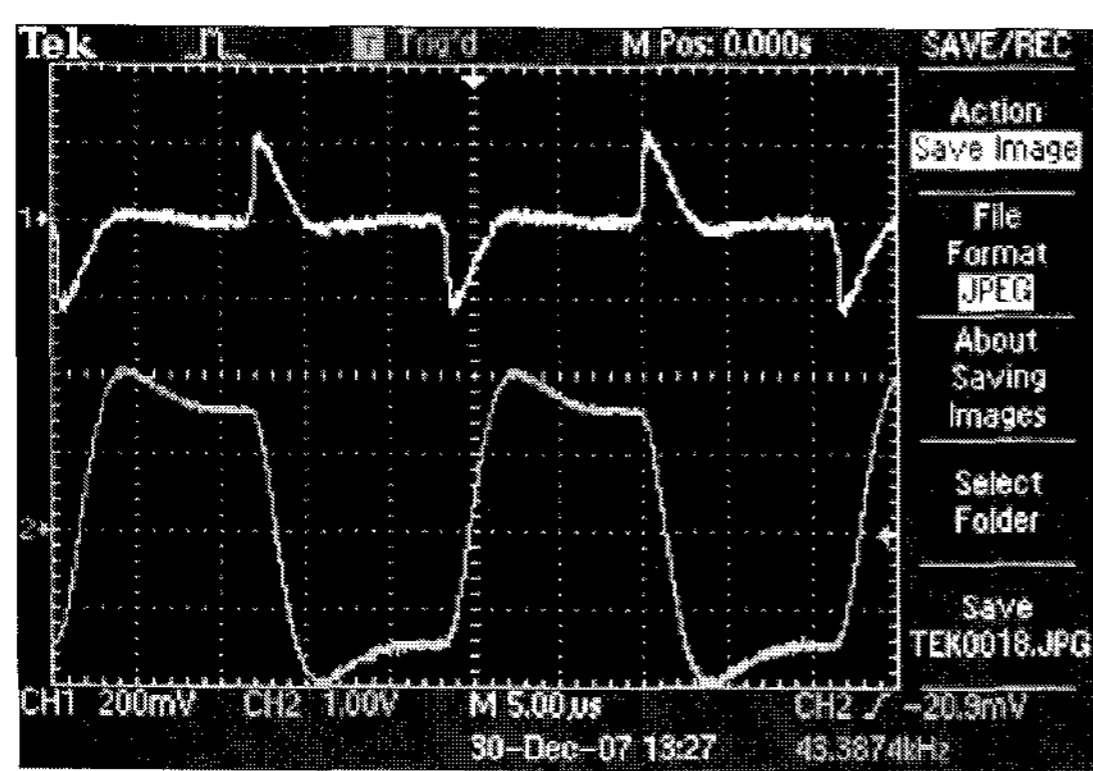


Fig. 10 Secondary Volt (B) & Current (Y), N L, $R_1=6.8\Omega$, $R_2=0.35\Omega$, $C=1\mu\text{F}$ Ceramic, $D=0.3$.

It is clear that the peak primary voltage is 20V with no overlapping between signals (Duty Cycle 45%), while the peak secondary voltage is 2V.

Fig. 11 and Fig. 12 show two B-H curves at different values for R_1 and no load transformer conditions.

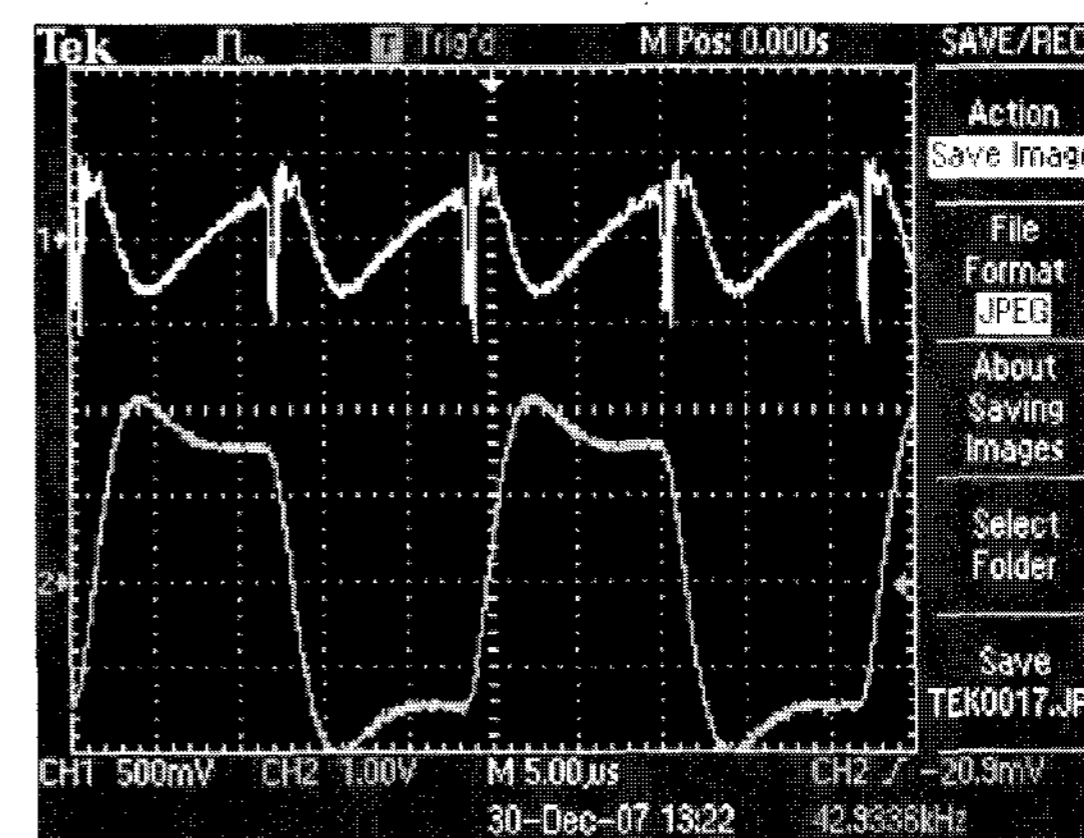


Fig. 13 Secondary Volt (B), Primary Current (Y), No Load, $R_1=0.35\Omega$, $R_2=6.8\Omega$, $C=1\mu\text{F}$ Ceramic, $D=0.45$

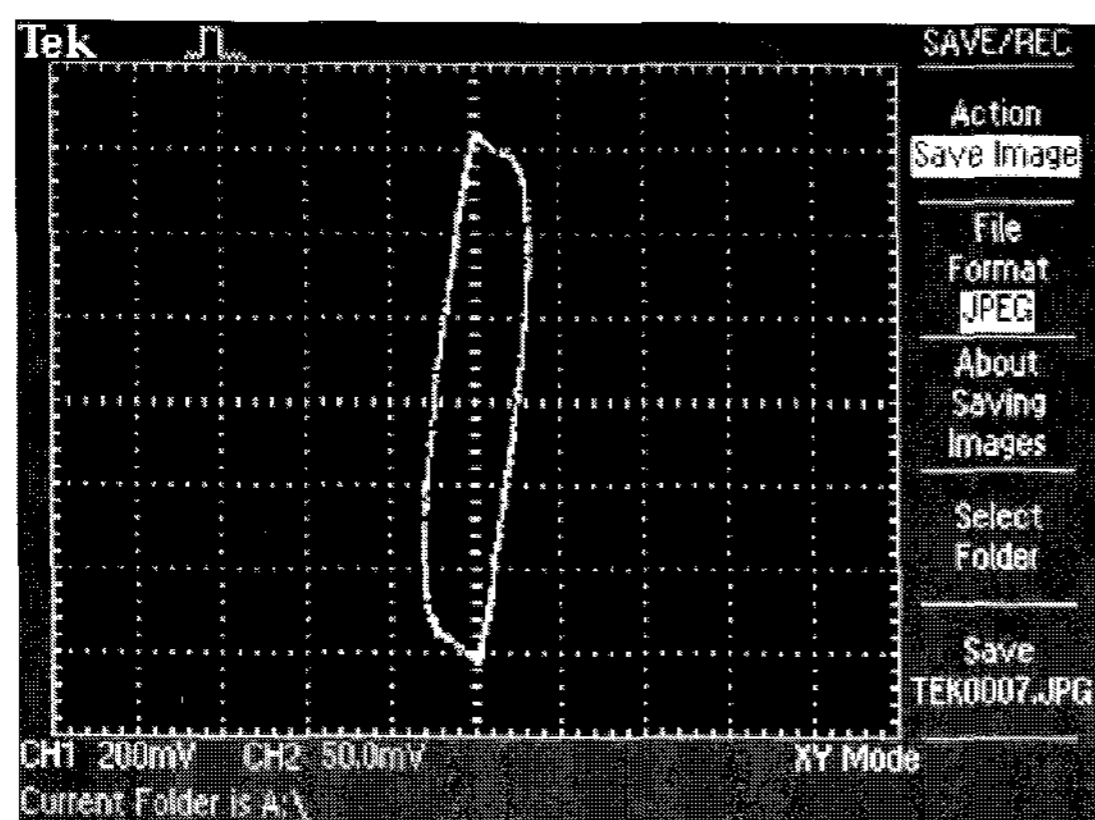


Fig. 11 B-H Curve, 45% Duty Cycle, $R_1=1\Omega$, $C=1\mu\text{F}$ Ceramic, No Load

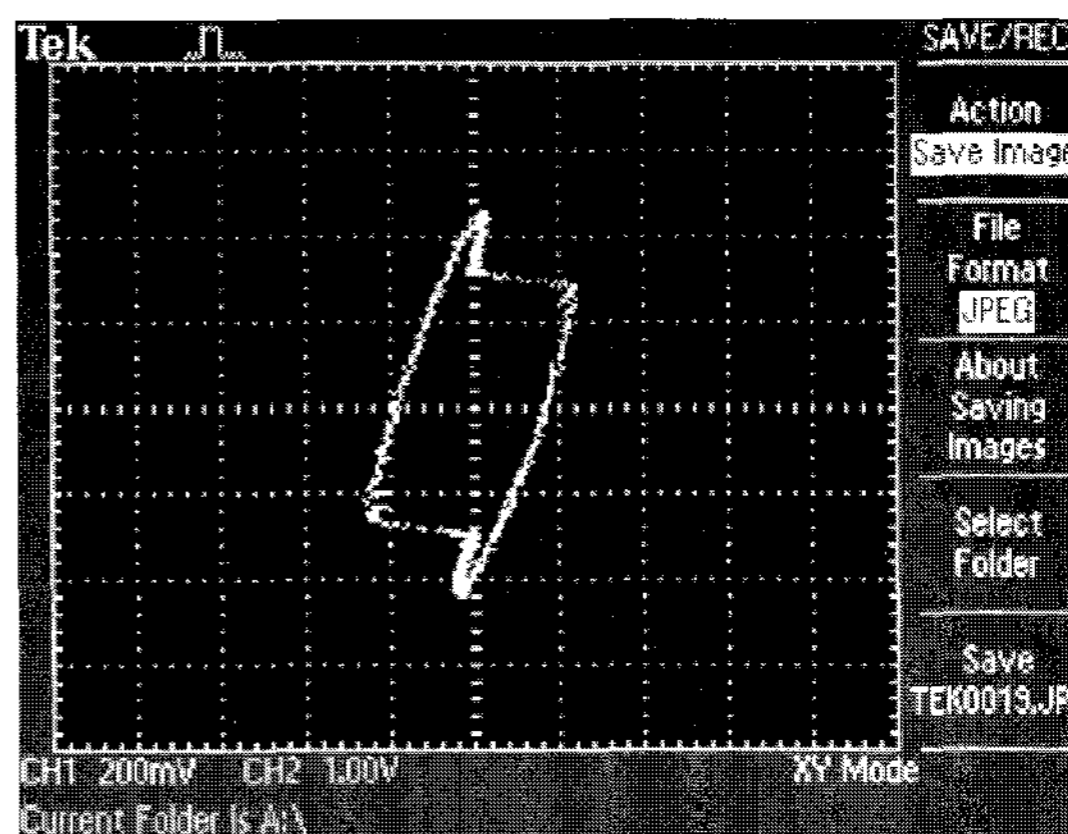


Fig. 14 B-H Curve at Conditions; $R_1=0.35\Omega$, $R_2=6.8\Omega$, $C=1\mu\text{F}$ ceramic

Fig. 15 shows the secondary voltage (Blue) and current (Yellow) while Fig. 16 shows the B-H curves at test conditions in Fig. 15 and transformer loading.

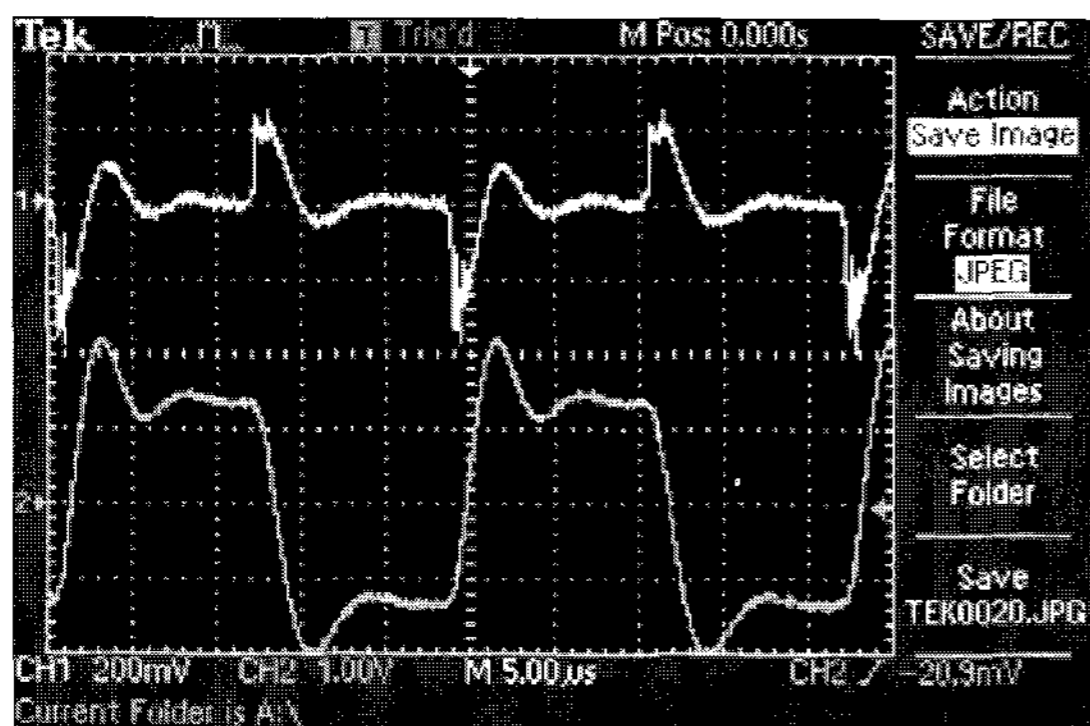


Fig. 15 Transformer Secondary Voltages (B) & Current (Y)

Fig. 17 shows the primary voltage (Blue) and current (Yellow) and Fig. 18 shows the secondary voltage (Blue) and current (Yellow) while secondary during a short circuit via rectifying diode loading conditions.

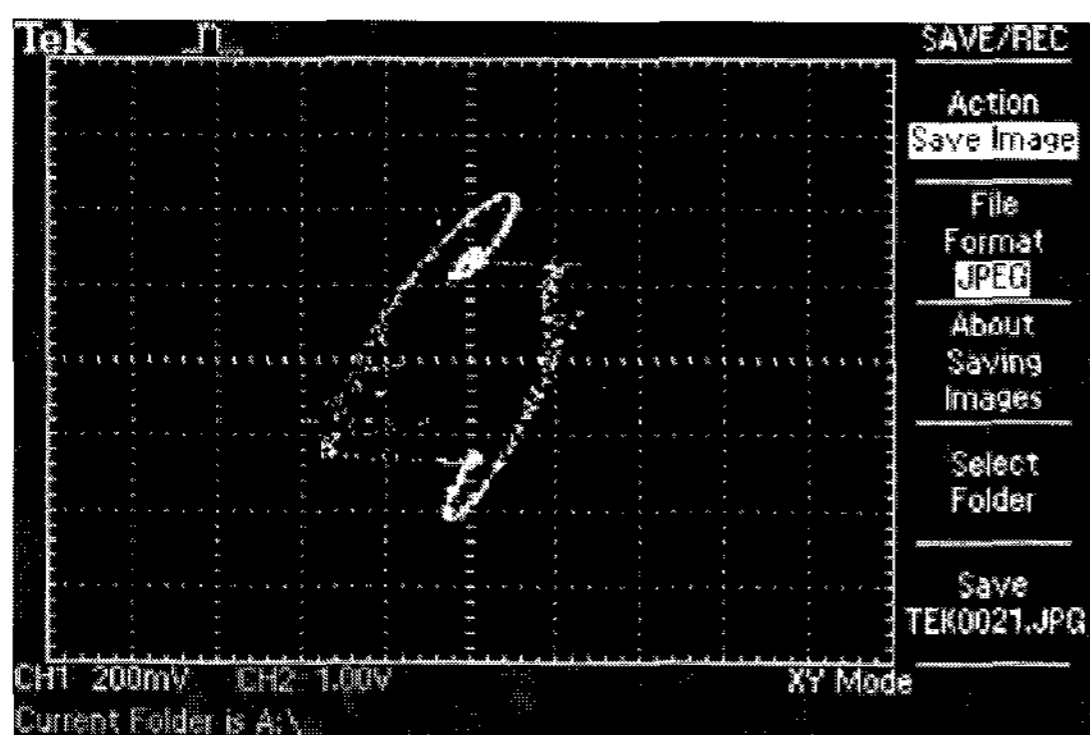


Fig. 16 B-H Curve of Conditions in Fig. 15

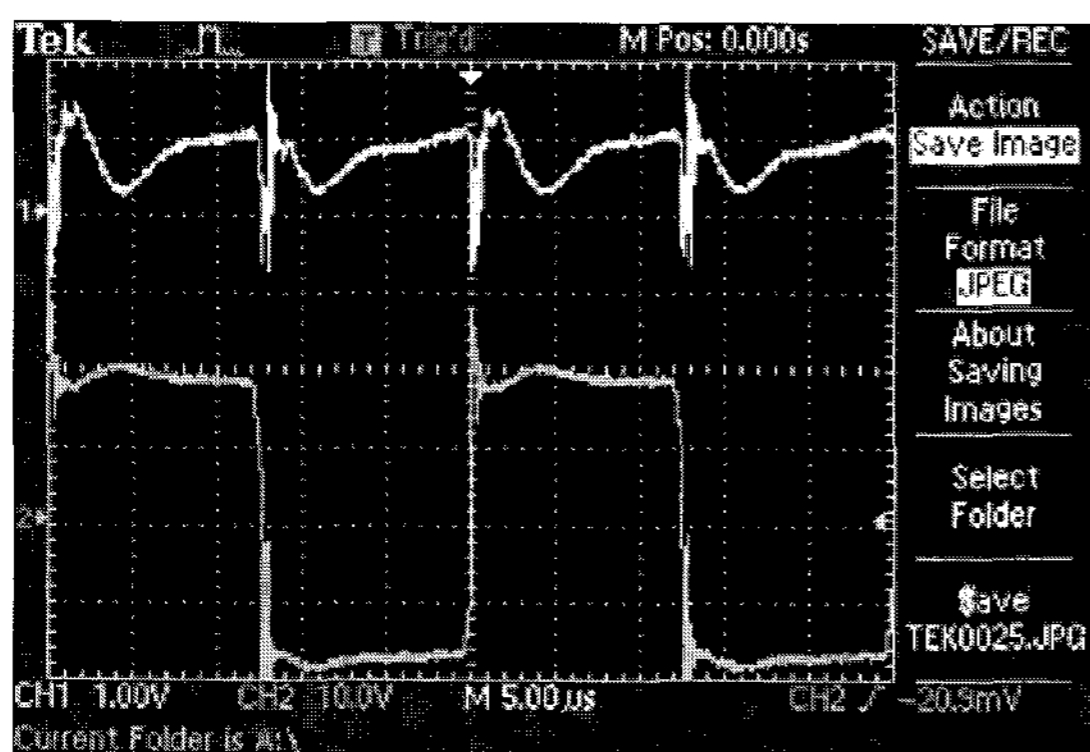


Fig. 17 Primary Current and Voltage, Loaded (DC)

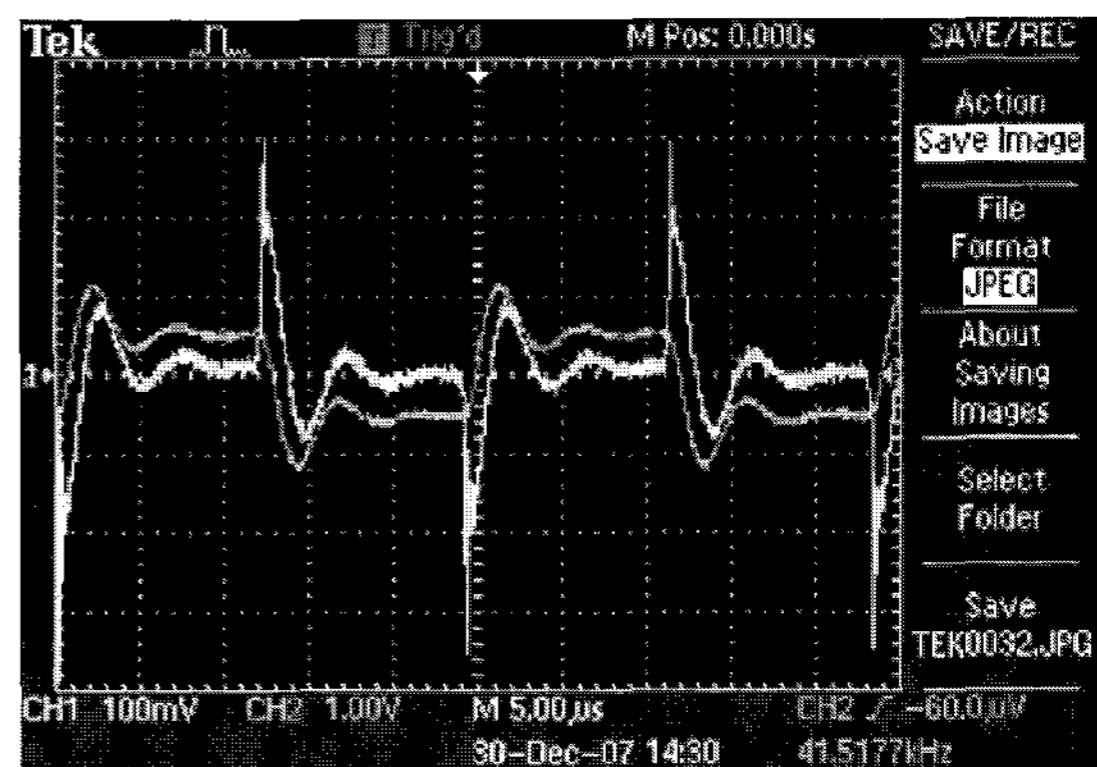


Fig. 18 Secondary Current and Voltage, at Short Circuit test (AC)

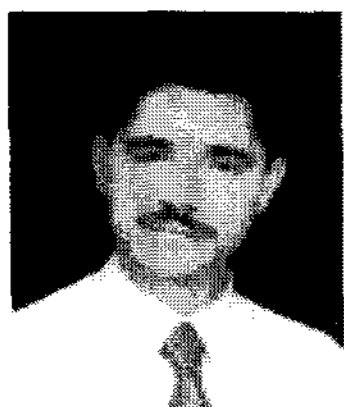
9. Conclusions

The design and implementation of an HF transformer for satellite EPS applications is introduced in this paper. The specifications for the transformer reflect the actual requirements for the battery charge equalization unit of the LEO satellite EPS. Two approaches for HF transformer design were applied; the analysis of the design results confirms that the first approach provided an appropriate design. The calculated and measured parameters of the implemented transformer were converged together. The hardware setup was built to test the implemented transformer waveforms and B-H curves at different operation conditions. The results prove that the transformer will not become saturated during the handling of the desired maximum power rating.

References

- [1] Colonel Wm. T. McLyman, "Inverter Transformer Core Design and Material Selection", Magnetics Division of Spang & Company, Spacecraft Power Section, Jet Propulsion Laboratory, Guidance and Control Division, 1999 Magnetics, www.mag-inc.com
- [2] Philips Semiconductors, "Design of HF wideband power transformers", *Application Note ECO6907*, <http://myweb.tiscali.co.uk/radiokits/radio-related/LinearPA/ECO6907.pdf>, Mar. 23, 1998.
- [3] COLONEL WM. T. MCLYMAN, "Transformer and Inductor Design Handbook, Third Edition, Revised and Expanded", ISBN: 0-8247-5393-3, Marcel Dekker, Inc. 270 Madison Avenue, New York, NY 10016, U.S.A., 2004.
- [4] Philips Components, "Applications, Soft Ferrites", Supersedes data of 1998 Mar 25, File under Ferrite

- Ceramics, MA01, Dec 23, 1999 & <http://www.ferroxcube.com/prod/assets/sfappl.pdf>, Sep. 1, 2004.
- [5] R.W. Erickson, "Fundamentals of Power Electronics", New York: Chapman and Hall (Kluwer Academic Publishers), May 1997. ISBN 0-412-08541-0, TK7881.15.E75 1997.
- [6] VOLTECHNOTES, "Transformer Basics", Voltech Instruments, Inc. 11637 Kelly Road, Suite 306 Fort Myers, FL 33908-2544 U.S.A. VPN 104-039/1, 2004.
- [7] L.G. Meares and Charles E. Hymowitz, "SPICE Models for Power Electronics", www.intusoft.com/articles/satcore.pdf
- [8] Jaroslav Dudrik, Juraj Oetter, "High-Frequency Soft-Switching DC-DC Converters for Voltage and Current DC Power Sources", *Acta Polytechnica Hungarica Journal*, Vol. 4, No. 2, 2007.
- [9] Mika Sippola, "Developments for the high frequency power transformer design and implementation", Helsinki University of Technology Applied Electronics Laboratory, Series E: Electronic Publications E3, Espoo 2003, <http://lib.tkk.fi/Diss/2003/isbn9512265877.pdf>
- [10] Tommy Kjellqvist, Staffan Norrga and Stefan O. stlund, "Design Considerations for a Medium Frequency Transformer in a Line Side Power Conversion System", 2004 35th Annual IEEE Power Electronics Specialists Conference Aachen, Germany, 2004.
- [11] STEWARD, "Ferrite Property Measurement", <http://www.steward.com/pdfs/cores/ferrprop.pdf>



Mohamed Bayoumy A. Zahran (M. Zahran) was born in Egypt, and received his B.Sc from Kima High Institute of Technology in 1987, M.Sc in 1993 and Ph.D. in 1999 from Cairo University, Faculty of Engineering, Electrical Power and Machines

Dept. He is an Associate Professor Researcher at the Electronics Research Institute, Photovoltaic Cells Dept. His experience is mainly in the field of renewable energy sources, systems design, management and control. He has been employed full time by the National Authority for Remote Sensing and Space Science (NARSS), Space Division, since 2002, as a System Engineer for the MisrSat-2 Project and as a Satellite Power Subsystem Designer.